Electronic structure of copper-rich copper-gold alloys

H. Asonen, C. J. Barnes,* M. Pessa, and R. S. Rao
Physics Department, Tampere University of Technology, SF-33101 Tampere 10, Finland

A. Bansil
Physics Department, Northeastern University, Boston, Massachusetts 02115
(Received 15 October 1984)

We present and discuss angle-resolved photoemission measurements from the (111) and (100) faces of *Cu*Au single crystals containing 10 at. % Au in the bulk, together with computations of complex-energy bands and densities of states in the $Cu_{90}Au_{10}$ random alloy. Our calculations permit a good understanding of the shifts and smearings in the spectrum of Cu arising from the addition of Au with respect to the Cu *d*-band complex, the (111) Shockley state, and the (100) Tamm state. The observed position and width of the Au-induced structure in the density of states is also in good accord with the theoretical result. Aspects of the electronic spectrum of *Cu*Au are compared and contrasted with those of *Cu*Al, *Cu*Pd, and *Cu*Ni solid solutions.

I. INTRODUCTION

The modern theory of disordered alloys predicts that the (real) Bloch energy levels of a perfect crystal will give rise to complex-energy bands in an alloy. These complex-energy bands represent the average properties of the system, their nonzero imaginary parts reflecting the disorder smearing of states. Angle-resolved photoemission spectroscopy (ARPES) has been used to probe individual energy levels in perfect crystals and more recently in disordered alloys,[1,2] making it possible for the first time to directly confront theory with experiment at perhaps one of the most fundamental levels. With this motivation, we have previously considered the bulk and surface electronic structures of *Cu*Al,[3–5] *Cu*Ge,[6] and *Cu*Pd (Ref. 7) alloys. This paper considers the case of the noble metal—noble metal system *Cu*Au. The ARPES results are compared with Korringa-Kohn-Rostoker coherent-potential-approximation (KKR-CPA) computations[1,2] on $Cu_{90}Au_{10}$. Our focus here will only be on the properties of *Cu*Au solid solutions containing Au concentrations well below 25 at. %, at which point the system undergoes the classic order-disorder transformation. The latter case will be discussed elsewhere.

A summary of our major conclusions is as follows. The changes in the electronic spectrum of Cu upon adding Au impurities are as follows. (i) Au induces broad, rather structureless features centered at about 6.4-eV binding energy (ranging from 5.5 to 7.2 eV). (ii) The Cu *d*-band complex suffers shifts of less than 0.3 eV. The states at the top of the Cu *d* band suffer little shifts, see little disorder scattering and behave like virtual crystal levels. (iii) The Shockley state of Cu(111) surface remains at the same binding energy of 0.35 eV and shows an increased broadening of about 70 meV. (iv) The changes in the binding energy and width of the (100) surface Tamm state of Cu are 150 and 80 meV, respectively. The nonrelativistic KKR-CPA computations on $Cu_{90}Au_{10}$ permit a good understanding of the various aforementioned effects. We compare and contrast aspects of the electronic spectrum of *Cu*Au with those of *Cu*Al, *Cu*Pd, and *Cu*Ni solid solutions. Finally, the good accord between the present nonrelativistic calculations and experiments indicates that at least in the present photoemission spectra, the relativistic effects are less apparent in *Cu*Au than in Au.

II. EXPERIMENTAL AND THEORETICAL CONSIDERATIONS

The experiments were performed using a multitechnique VG ADES 400 spectrometer, with *in situ* facilities for low-energy electron diffraction (LEED), Auger-electron spectroscopy (AES), ARPES, and x-ray photoelectron spectroscopy (XPS) measurements. He I (21.22 eV), He II (40.82 eV), Ne I (16.85 eV), and Ne II (26.9 eV) resonance lines from a gas-discharge lamp were used to induce electron emission. The *Cu*Au single crystals were grown by the Bridgman method. X-ray fluorescence measurements indicated the bulk composition to be $Cu_{90}Au_{10}$. The samples were cleaned by repeated cycles of Ar^+-ion bombardment and annealing. Due to the large atomic size difference between Cu and Au, surface enrichment of Au is expected. Since Ar^+-ion bombardment again leads to Au enrichment due to preferential sputtering of Cu, care was taken to prepare each surface studied in an identical fashion. Our AES estimate is that the outermost surface layer contains an Au concentration of about 20 at. %. The second and subsequent layers are assumed to be close to the bulk Au concentration of 10 at. % on the basis of surface concentration studies of disordered *Cu*Au alloys available in literature.[8] LEED studies showed the (111) surface to be of high (1×1) structural perfection, while the (100) surface indicated the presence of small areas of a $(\sqrt{2}\times\sqrt{2}R45°)$ superstructure.[9]

The theoretical techniques used in the present KKR-CPA calculations are summarized in Ref. 2, to which we refer also for other relevant references. Cu and Au

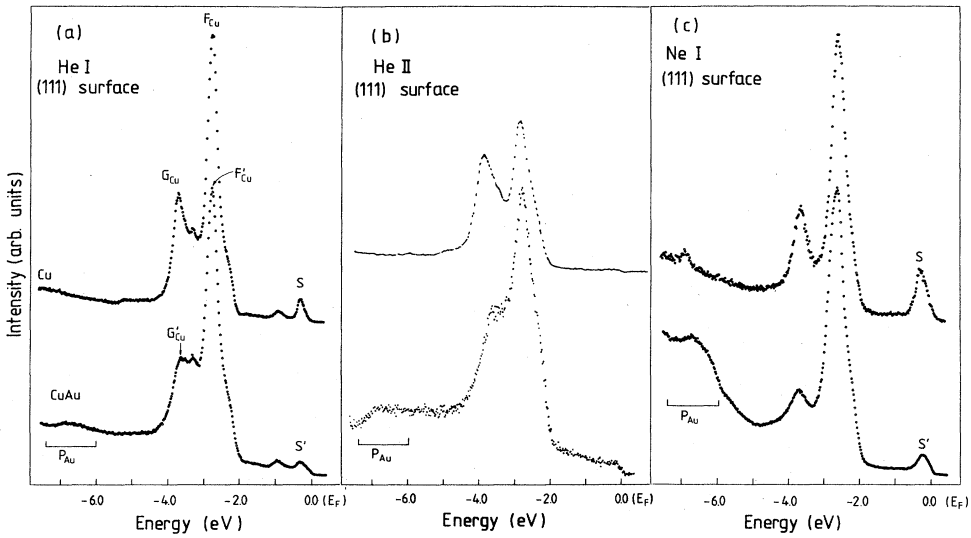

FIG. 1. He I, He II, and Ne I angle-resolved normal-emission spectra from the (111) surface of Cu and *Cu*Au. The Cu- and Au-derived structure, identified by various letters, are discussed in the text.

muffin-tin potentials were obtained via the Mattheiss overlapping charge densities prescription. An fcc lattice of lattice constant 6.933 a.u. appropriate for the $Cu_{90}Au_{10}$ alloy was employed. Herman-Skillman wave functions for atomic configuration of $3d^{10}4s^1$ for Cu, and Liberman charge densities for the $5d^{10}6s^1$ configuration of Au were used. The Cu potential is identical to the one used in our recent study of *Cu*Pd alloys.[7] The Au potential obtained for the alloy lattice constant was shifted rigidly to a lower energy by 0.18 Ry with respect to the Cu potential. This is the only semiempirical adjustment invoked for the Au potential. This adjustment may be viewed as a means of incorporating the effects of charge rearrangement upon alloying. The present computations are nonrelativistic, while the relativistic spin-orbit interaction is known to be important in Au.[10] The overall good agreement between the theory and experiment indicates nevertheless that at least in the Cu-rich alloy with Au the relativistic effects are less apparent in the photoemission spectra. We further comment on this point below.

III. RESULTS AND DISCUSSION

He I, He II, and Ne I normal-emission spectra from the (111) and (100) faces are compared in Figs. 1 and 2 for Cu and *Cu*Au single crystals. (Ne II spectra are not shown as structures due to satellite frequencies in the uv source overlap with the primary Ne II spectra.) These results will be interpreted in terms of the alloy complex-energy-band calculation on $Cu_{90}Au_{10}$ and the associated densities of states of Figs. 3 and 4. With reference to the (111) He I spectra in Fig. 1, the typical effects of adding Au to Cu

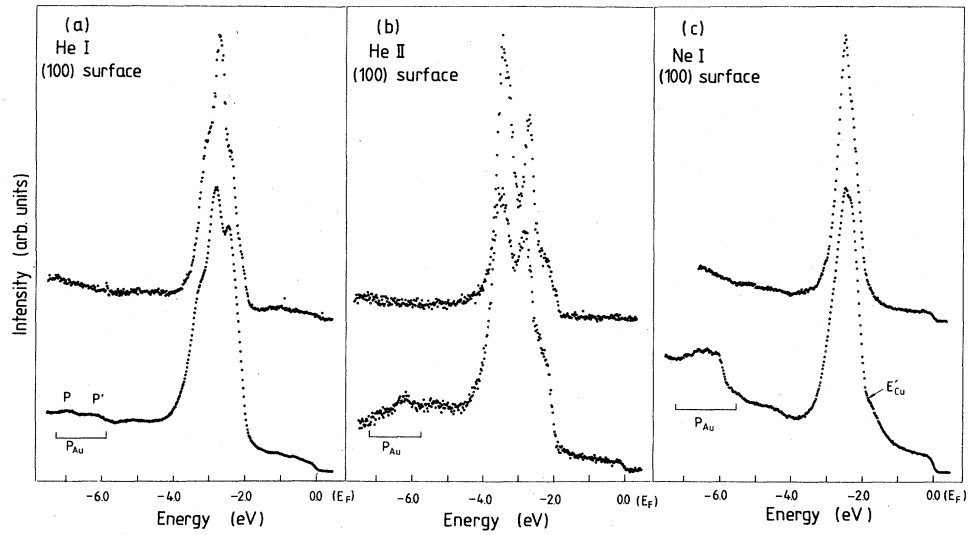

FIG. 2. Same as Fig. 1, except that this figure refers to the (100) surface.

are seen to be (i) the Cu-derived peaks, e.g., F'_{Cu} and G'_{Cu} show an increased smearing but little shift in energy, (ii) Au induces broad new structures, P_{Au}, between 5.5- and 7.2-eV binding energies, (iii) the (111) Shockley surface state S', although somewhat more smeared, shows little shift in energy. Similar differences are also seen between the other, Cu and *Cu*Au spectra in Figs. 1 and 2.

A quantitative comparison between the theoretical and experimental results is made in Figs. 3 and 4. With four different uv frequencies we were able to probe a fairly large part of the Brillouin zone. The E-**k** values for the Cu-derived peaks[11] (crosses) are in good accord with the theoretical bands, as is the measured position and width of Au-induced structure (cross-hatched). The calculated Au d bands possess little dispersion but large dampings (on the order of 1 eV) and thus the associated density of states (Fig. 4) is structureless. These theoretical predictions are consistent with our experiments in that we find the Au-induced feature to show little change between different crystal faces or for different uv frequencies. The top of the Cu d band sees little disorder smearing; for example, in the case of the peak F_{Cu} in Fig. 1, the measured increase in the full width at half-maximum[12] (FWHM) of F'_{Cu} is less than 60 meV, as is the calculated disorder smearing for the corresponding E-**k** point in the alloy. In contrast, the bottom of the Cu d band is more smeared. By measuring the FWHM of the peaks G_{Cu} and G'_{Cu}, for example, we estimate an increase of 150 meV, in agreement with the associated calculated value of 130 meV. This difference between the behavior of the top and bottom of the Cu d bands is probably a subtle effect and we return to this point below.

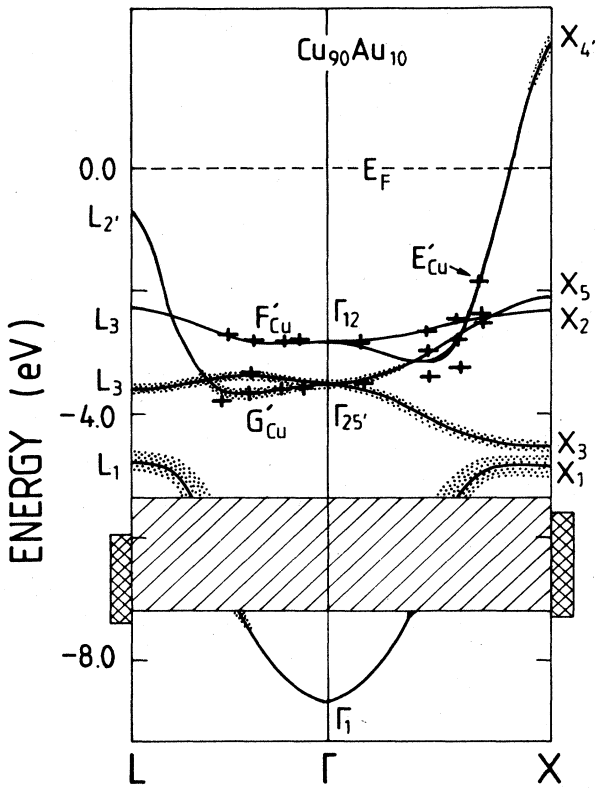

FIG. 3. Complex energy bands in $Cu_{90}Au_{10}$ along the symmetry directions Γ—L and Γ—X. Vertical length of shading around the bands equals 2 times the imaginary parts of the complex energies. Heavily smeared Au-related d bands are shown as hatched region of full width at half maximum of the Au-site peak in Fig. 4. Crosses give the $E(\mathbf{k})$ values obtained from the experimental spectra (levels labeled F'_{Cu}, G'_{Cu}, and E'_{Cu} refer to corresponding spectral features of Figs. 1 and 2). The cross-hatched regions around the L and X points give the range in which the Au-induced structures are seen in the spectra of Figs. 1 and 2, respectively.

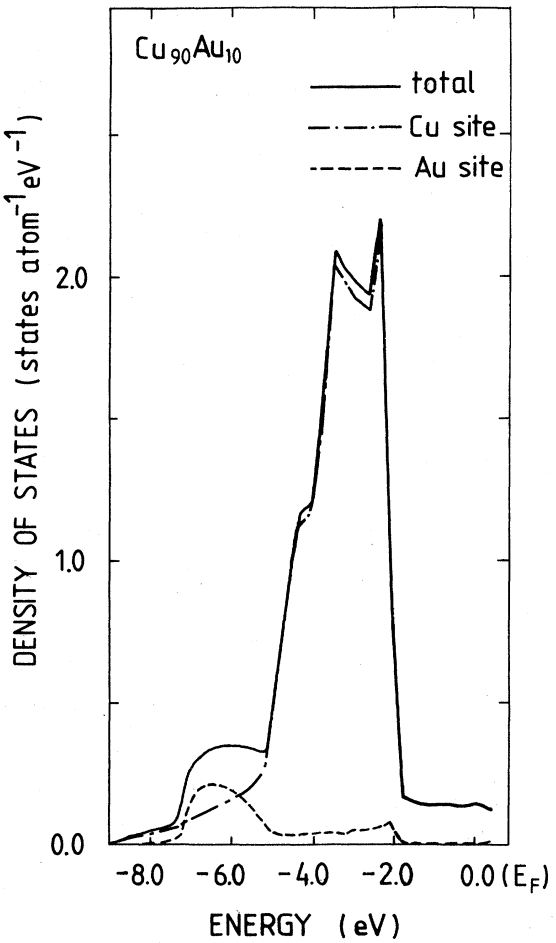

FIG. 4. Average density of states in $Cu_{90}Au_{10}$, together with the components of the density of states associated with Cu and Au sites.

Insight into the nature of the electronic spectrum of the *Cu*Au system is provided by Fig. 5 which compares the typical energy bands in Cu and Au, and also in Cu and Ni. These bands are based on the Cu, Au, and Ni muffin-tin potentials relevant to the *Cu*Au and *Cu*Ni (Ref. 13) alloys and do not represent any real crystals. They are very useful nevertheless because they permit an understanding of the main features of the alloy spectrum in simple terms. In Fig. 5(a) the centers as well as the bottoms of the Cu and Au d bands (e.g., Δ'_2) are well separat-

ed and would give two sets of levels in the alloy. The tops of the Cu and Au d bands, in contrast, intersect (e.g., Δ_2 and Δ_5) and therefore the states in that energy regime will behave as if they were in a virtual crystal and suffer little disorder damping. For this reason, the top of the d band in *Cu*Au spectra in Figs. 1 and 2 really represent mixed Cu-Au alloy states. This effect is also reflected in the fact that the Au component density of states in Fig. 4 contains substantial weight near the top of Cu d band around -2.1 eV. The aforementioned phenomenon is the result of delicate interplay between the relative positions and widths of the Cu and Au d bands. For instance, if the Au d band was much narrower than in Fig. 5(a), the tops of the Cu and Au d bands would have split into two, like the rest of the d band complex. On the other hand, if the Au d band were much broader than in Fig. 5(a), the d band would have split and appeared above the Cu d band, much like the situation in *Cu*Pd.[7] The case of *Cu*Au is to be contrasted with that of *Cu*Ni, where all the Cu and Ni d bands are well split [Fig. 5(b)]. Finally, we note that s-p—type levels of Cu and Au (e.g., X_4') yield a common band in *Cu*Au as well as in *Cu*Ni because the separation between these bands is small compared to the typical bandwidth of the order of a Rydberg for the free-electron bands. The preceding discussion makes it clear that while Fig. 6 appears to show that Au and Ni essentially give rise to a virtual bound state in Cu (of course, the Au resonance lies below the Cu d-band complex while the Ni resonance lies above it), there are more subtle effects which arise from the larger width of the Au d band in comparison to that of Ni.

A few brief comments concerning the neglect of relativistic effects in our calculations are appropriate here. As noted above, these effects are known to be important in pure Au (Ref. 10) and in some Au alloys,[14] where they split the Au d-band density of states into two structures, ≈ 2.5 eV apart.[10] We emphasize, however, that the situation of an Au atom in *Cu*Au differs substantially from that of pure Au. The lattice size of $Cu_{90}Au_{10}$ is about 9.7% less than that of Au, leading to a 65% increase in the effective width of the d band in *Cu*Au [using X_5-X_1 as a measure, the values are as follows: Au, 6.1 eV; Au on $Cu_{90}Au_{10}$ lattice, Fig. 5(a), 10 eV]. Furthermore, the Au levels suffer disorder smearings on the order of 1 eV in $Cu_{90}Au_{10}$. The increased d band width and disorder smearing would both act to smooth the influence of any relativistic splitting in *Cu*Au. In any event, the calculated Au d-band peak between -5.0 and -7.2 eV (Fig. 4) is in good accord with the observed gold-induced features in the binding-energy range from ≈ 5.5 to ≈ 7.2 eV, and like the theoretical Au density of states in Figs. 4 and 6, these spectral features in Figs. 1 and 2 do not contain much structure. Smaller features seen in some of the spectra may be due to some dispersion still remaining in the Au d-band complex in the alloy. However, we cannot exclude the possibility that the two distinct peaks P and P' (≈ 0.7 eV apart) in Fig. 2(a) may correspond to relativistic splitting of the Au density of states; but such a splitting is less apparent in the other spectra.

Focusing attention now on surface states, we consider in Fig. 7 the (111)-surface Shockley state S'. *Cu*Al and *Cu*Pd data are reproduced in Fig. 7 from Refs. 3 and 7 in order to compare and contrast the alloying effects on S' in different Cu-based solid solutions. In Fig. 7 the measured changes in the position of the Shockley state compared to Cu are as follows: *Cu*Au, no change;[15] *Cu*Pd, 200 meV; *Cu*Al, -400 meV (the negative sign denotes a shift to higher binding energy in relation to Cu). We have previously argued[3] that since this surface state resides in the L_2'—L_1^u gap in the spectrum, its behavior can be un-

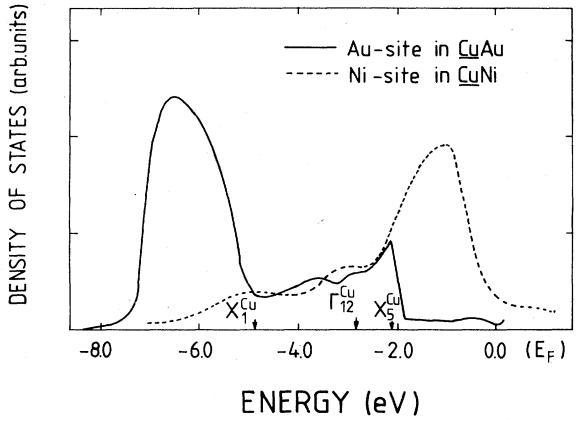

FIG. 6. Density of states associated with a Au site in *Cu*Au and the corresponding result for a Ni site in *Cu*Ni [from Fig. 8(a) in Ref. 13]. The positions of the typical Cu d levels in *Cu*Au are shown on the energy axis. Γ_{12}^{Cu} levels in *Cu*Au and *Cu*Ni are aligned for comparison. (Vertical scales for Au and Ni are not the same.)

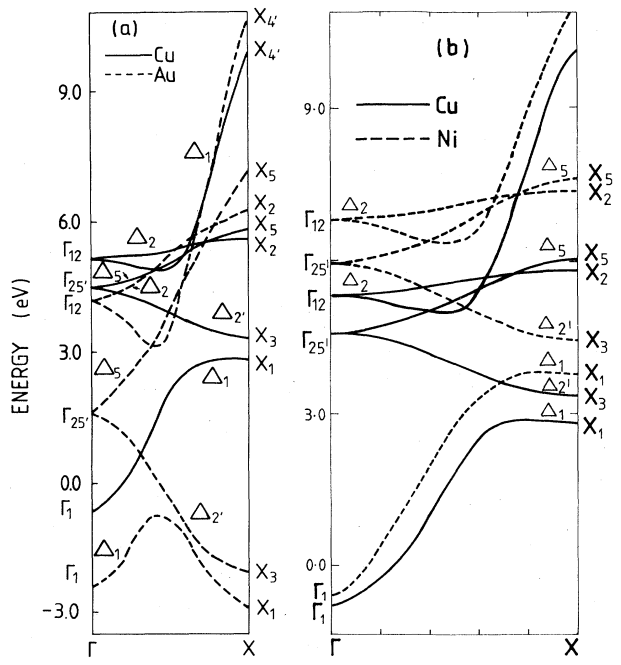

FIG. 5. (a) Γ—X energy bands for hypothetical Cu and Au crystals using the potentials used in the $Cu_{90}Au_{10}$ computations. (b) Similarly compares the Cu and Ni bands relevant for the *Cu*Ni system.

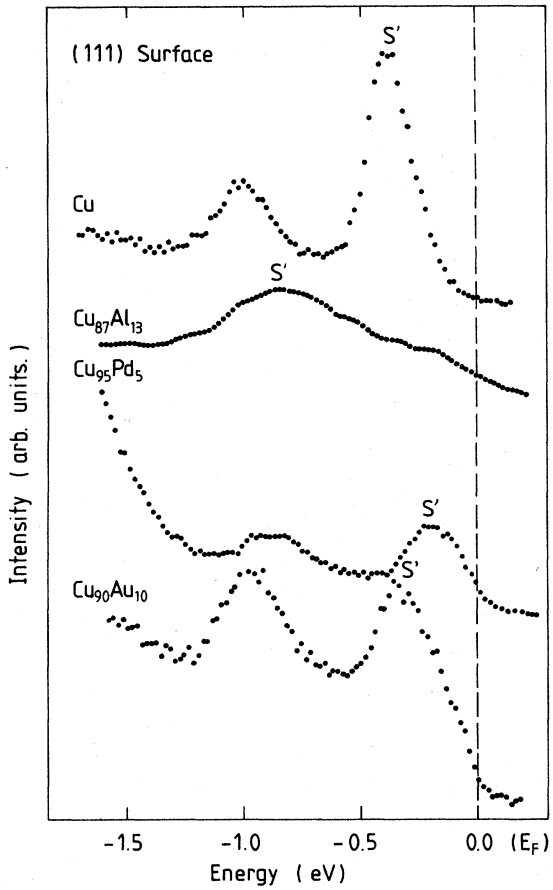

FIG. 7. Normal-emission spectra for the (111) surface are shown on an expanded scale in the energy region of the $\bar{\Gamma}$-centered Shockley state S' in Cu, *Cu*Al, *Cu*Pd, and *Cu*Au. Ne I spectrum is shown for *Cu*Al and the rest are He I spectra. The structure at ≈ -1.0 eV is due to satellite frequency in the He I source.

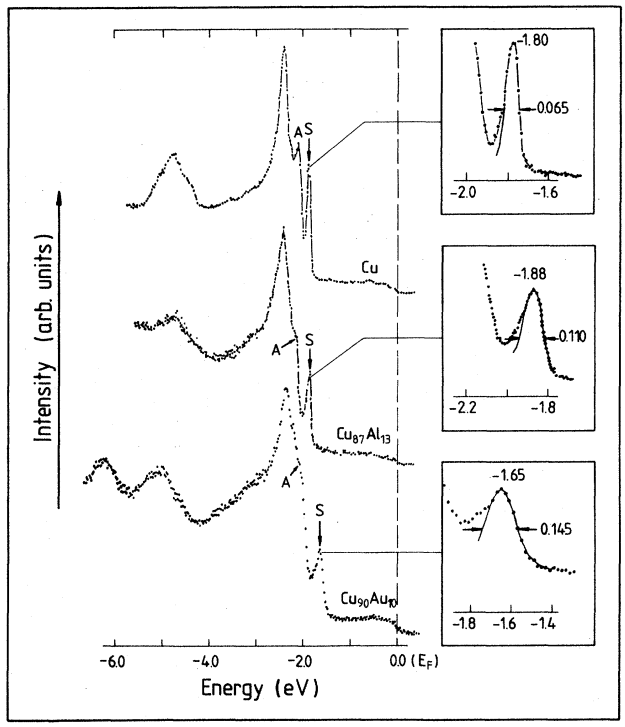

FIG. 8. He I spectra displaying the (100)-surface Tamm states S in Cu, *Cu*Al, and *Cu*Au. The insets show the peak S on an expanded scale. All the spectra are from the (100) faces for a polar emission angle of 63°. Peak A arises from bulk transition near the top of the Cu d-band complex.

derstood in terms of these bulk levels. The Cu $L_2'-L_1^u$ gap shows little change on alloying in *Cu*Au and *Cu*Pd,[7] and the corresponding calculated shifts in L_2' or the center of the $L_2'-L_1^u$ gap are as follows: $Cu_{90}Au_{10}$, no shift; $Cu_{95}Pd_5$, 160 meV. In *Cu*Al, however, the $L_2'-L_1^u$ gap decreases with solute concentration[16] and hence, relating the shift and smearing of S' to bulk levels becomes less clear. The calculated shifts (with respect to Fermi energy) of L_2' and L_1^u levels in $Cu_{87}Al_{13}$ are -0.98 and -1.78 eV, respectively, giving an average shift of -1.38 eV for the center of the gap. Regarding the broadening of the Cu Shockley state, observed increases (Fig. 7) in the FWHM are as follows: *Cu*Au, 70 meV; *Cu*Pd, 60 meV; *Cu*Al, ≈ 100 meV or less [estimated by the broadening of S' for $(\sqrt{3}\times\sqrt{3}R30°)$ surface as the Ar^+-ion bombardment, employed to obtain the regular (1×1) surface (see Ref. 3), induces additional broadening]. Again in *Cu*Au and *Cu*Pd the computed disorder smearings of the L_2' and L_1^u levels are comparable and reasonably small (about 100 meV or less). The average smearing of the L_2' and L_1^u levels are 80 meV for $Cu_{90}Au_{10}$ and 45 meV for $Cu_{95}Pd_5$ and are of the same order of magnitude as the experimental values for S' quoted above. But in *Cu*Al the computed disorder smearing of a bulk level varies significantly with energy, and for the L_1^u level it is an order of magnitude larger than that of L_2' level. The Shockley state lies closer to L_2' than L_1^u, and its observed broadening in $Cu_{87}Al_{13}$ agrees better with the computed L_2'-level smearing of 130 meV. In any case, the reason the Shockley state is more smeared in *Cu*Al compared to *Cu*Pd or *Cu*Au is that the s-p levels of Cu suffer larger scattering upon alloying with Al in comparison to Pd or Au. Similarly, the L_2' level shows little shift with respect to Fermi level in *Cu*Au and so does the surface state S',[17,18] the shift in *Cu*Pd being larger.

Figure 8 compares the (100)-surface Tamm state in Cu, *Cu*Al (from Ref. 4 for comparison), and *Cu*Au. This surface state is not observable in *Cu*Pd (see Ref. 7) due to strong emission from the Pd d bands in its energy range. Its presence in our spectra suggests the absence of substantial Au-induced states above the Cu d bands in *Cu*Au. The Tamm state is well known to be split off the top of the Cu d band as a result of the surface perturbation. Therefore, in Ref. 4 we associated the properties of this state with those of the bulk d bands near the top of the d-band complex, and were able to provide some understanding of the measurement on *Cu*Al. Here in the case of *Cu*Au, the observed increase in FWHM of peak S (Fig. 8) is 80 meV, whereas the calculated disorder smearing of

the bulk states at the top of the Cu d-band complex is 35 meV. The discrepancy may be attributed to the Au enrichment of the topmost layer; but may partly be due to poorer (1×1) structural quality of the *Cu*Au(100) surface compared to that of Cu(100) (see Sec. II above). (Linear extrapolation of the computed smearing to 20 at.% Au would give 70-meV broadening.) Regarding the position of the Tamm state, the peaks S and A in Fig. 8 are 420 meV apart for *Cu*Au as compared to 280 meV for *Cu*Al (Ref. 4) and 180 meV for Cu. The increased separation of the Tamm state from the bulk d-band edge indicates greater deviation of the surface atom potential from the bulk potential; this effect having been enhanced by the Au enrichment at the topmost surface layer. Note that Tamm state arises due to strong changes in the potential at the surface, whereas Shockley state could arise due to mere termination of the crystal. Therefore the Tamm state would be more sensitive to the surface enrichment in *Cu*Au than the Shockley state, in accordance with our discussion above.

ACKNOWLEDGMENTS

We acknowledge the technical assistance of Mr. A. Vuoristo and Mr. A. Salokatve. Financial assistance of the U. S. National Science Foundation and the Academy of Finland is acknowledged.

---

*Present address: Donnan Laboratories, University of Liverpool, Liverpool L69 3BX, England.

[1]For recent reviews, see A. Bansil and M. Pessa, Phys. Scr. **T4**, 52 (1983) and Ref. 2 below.

[2]A. Bansil, in *Positron Annihilation,* edited by P. G. Coleman, S. C. Sharma, and L. Diana (North-Holland, Amsterdam, 1982), p. 291.

[3]H. Asonen, M. Lindroos, M. Pessa, R. Prasad, R. S. Rao, and A. Bansil, Phys. Rev. B **25**, 7075 (1982).

[4]M. Pessa, H. Asonen, R. S. Rao, R. Prasad, and A. Bansil, Phys. Rev. Lett. **47**, 1223 (1981).

[5]H. Asonen and M. Pessa, Phys. Rev. Lett. **46**, 1696 (1981).

[6]A. Bansil, R. S. Rao, R. Prasad, H. Asonen, and M. Pessa, J. Phys. F **14**, 273 (1984).

[7]R. S. Rao, A. Bansil, H. Asonen, and M. Pessa, Phys. Rev. B **29**, 1713 (1984).

[8]T. M. Buck, G. H. Wheatley, and L. Marchut, Phys. Rev. Lett. **51**, 43 (1983).

[9]Note that the lattice constant of $Cu_{80}Au_{20}$ is 7.04 a.u., which is 1.5% larger than that of $Cu_{90}Au_{10}$. With so small lattice mismatch, the enriched surface monolayer will be expected to take up the lattice constant of the bulk. Hence our LEED spots would not yield information about surface enrichment.

[10]N. E. Christensen, J. Phys. F **8**, L51 (1978); D. L. Weissman-Wenocur, P. M. Stefan, B. B. Pate, M. L. Shek, I. Lindau, and W. E. Spicer, Phys. Rev. B **27**, 3308 (1983).

[11]Assuming a free-electron final-state band, the E-$\mathbf{k}$ relations are obtained for Cu by the equation $|\mathbf{k}^f|(A^{-1}) = 0.4857(E_k+13.6)^{1/2}$ for the final state $\mathbf{k}^f$ *inside* the crystal to the final state kinetic energy (E_k) of the electron *outside* the crystal. We have found that this relation is very accurate for Cu in the low-energy uv region, which however needs to be modified for $Cu_{90}Au_{10}$. Here we obtained the $\mathbf{k}$ value for the E'_{Cu} peak (Ne I spectra) of Fig. 2 by using the calculated bands. (As the E-$\mathbf{k}$ dispersion of this s-p band is large, the error in this evaluation should be very small.) We have estimated that the changes $\Delta\mathbf{k}^f$ from the Cu values $\mathbf{k}^f$ (calculated by the equation mentioned above) satisfy $(\Delta\mathbf{k}^f)/\mathbf{k}^f = \text{const}$, to a very good approximation (from Ne I to He II incident photon energy range). Hence the Cu $\mathbf{k}^f$ values have been shifted accordingly for $Cu_{90}Au_{10}$.

[12]Contributions from the instrumental broadening have been subtracted from the measured FWHM of the observed spectral peaks by using Eq. (8) of O. Keski-Rahkonen and M. O. Krause, Phys. Rev. A **15**, 959 (1977).

[13]See A. Bansil, Phys. Rev. B **20**, 4035 (1979).

[14]P. Weinberger, J. Stauton, and B. L. Gyorffy, J. Phys. F **12**, 2229 (1982).

[15]Note that the accuracy of the measured positions is about ±50 meV.

[16]R. S. Rao, R. Prasad, and A. Bansil, Phys. Rev. B **28**, 5762 (1983).

[17]In our experiments (unpublished) on $Cu_{75}Au_{25}$ also, only a small shift for the (111) surface Shockley state is observed. Reference 18 also reports very little shift for this surface state in Cu_3Au.

[18]R. G. Jordan and G. S. Sohal, J. Phys. C **15**, L663 (1982).